

A comparative genomics multitool for scientific discovery and conservation

<https://doi.org/10.1038/s41586-020-2876-6>


Zoonomia Consortium*

Received: 17 April 2019

Accepted: 27 July 2020

Published online: 11 November 2020

Open access

 Check for updates

The Zoonomia Project is investigating the genomics of shared and specialized traits in eutherian mammals. Here we provide genome assemblies for 131 species, of which all but 9 are previously uncharacterized, and describe a whole-genome alignment of 240 species of considerable phylogenetic diversity, comprising representatives from more than 80% of mammalian families. We find that regions of reduced genetic diversity are more abundant in species at a high risk of extinction, discern signals of evolutionary selection at high resolution and provide insights from individual reference genomes. By prioritizing phylogenetic diversity and making data available quickly and without restriction, the Zoonomia Project aims to support biological discovery, medical research and the conservation of biodiversity.

The genomics revolution is enabling advances not only in medical research¹, but also in basic biology² and in the conservation of biodiversity, where genomic tools have helped to apprehend poachers³ and to protect endangered populations⁴. However, we have only a limited ability to predict which genomic variants lead to changes in organism-level phenotypes, such as increased disease risk—a task that, in humans, is complicated by the sheer size of the genome (about three billion nucleotides)⁵.

Comparative genomics can address this challenge by identifying nucleotide positions that have remained unchanged across millions of years of evolution⁶ (suggesting that changes at these positions will negatively affect fitness), focusing the search for disease-causing variants. In 2011, the 29 Mammals Project⁷ identified 12-base-pair (bp) regions of evolutionary constraint that in total comprise 4.2% of the genome, by measuring sequence conservation in humans plus 28 other mammals. These regions proved to be more enriched for the heritability of complex diseases than any other functional mark, including coding status⁸. By expanding the number of species and making an alignment that is independent of any single reference genome, the Zoonomia Project was designed to detect evolutionary constraint in the eutherian lineage at increased resolution, and to provide genomic resources for over 130 previously uncharacterized species.

Designing a comparative-genomics multitool

When selecting species, we sought to maximize evolutionary branch length, to include at least one species from each eutherian family, and to prioritize species of medical, biological or biodiversity conservation interest. Our assemblies increase the percentage of eutherian families with a representative genome from 49% to 82%, and include 9 species that are the sole extant member of their family and 7 species that are critically endangered⁹ (Fig. 1): the Mexican howler monkey (*Alouatta palliata mexicana*), hirola (*Beatragus hunteri*), Russian saiga (*Saiga tatarica tatarica*), social tuco-tuco (*Ctenomys sociabilis*), indri (*Indri indri*), northern white rhinoceros (*Ceratotherium simum cottoni*) and black rhinoceros (*Diceros bicornis*).

We collaborated with 28 institutions to collect samples, nearly half (47%) of which were provided by The Frozen Zoo of San Diego Zoo Global (Supplementary Table 1). Since 1975, The Frozen Zoo has stored renewable cell cultures for about 10,000 vertebrate animals that represent over 1,100 taxa, including more than 200 species that are classified as vulnerable, endangered, critically endangered or extinct by the International Union for Conservation of Nature (IUCN)¹⁰. For 36 target species we were unable to acquire a DNA sample of sufficient quality, even though our requirements were modest (Methods), which highlights a major impediment to expanding the phylogenetic diversity of genomics.

We used two complementary approaches to generate genome assemblies (Extended Data Table 1). First, for 131 genomes we generated assemblies by performing a single lane of sequencing (2× 250-bp reads) on PCR-free libraries and assembling with DISCOVAR de novo¹¹ (referred to here as 'DISCOVAR assemblies'). This method does not require intact cells and uses less than two micrograms of medium-quality DNA (most fragments are over 5 kilobases (kb) in size), which allowed us to include species that are difficult to access (Extended Data Figs. 1, 2) while achieving 'contiguous sequences constructed from overlapping short reads' (contig) lengths comparable to those of existing assemblies (median contig N50 of 46.8 kb, compared to 47.9 kb for Refseq genome assemblies).

For nine DISCOVAR assemblies and one pre-existing assembly (the lesser hedgehog tenrec (*Echinops telfairi*)), we increased contiguity 200-fold (the median scaffold length increased from 90.5 kb to 18.5 megabases (Mb)) through proximity ligation, which uses chromatin interaction data to capture the physical relationships among genomic regions¹². Unlike short-contiguity genomes, these assemblies capture structural changes such as chromosomal rearrangements¹³. The upgraded assemblies increase the number of eutherian orders that are represented by a long-range assembly (contig N50 > 20 kb and scaffold N50 > 10 Mb) from 12 to 18 (out of 19). We are working on upgrading the assembly of the large treeshrew (*Tupaia tana*) for the remaining order (Scandentia).

Comparative power of 240 species

The Zoonomia alignment includes 120 newly generated assemblies and 121 existing assemblies, representing a total of 240 species (the

*A list of authors and their affiliations appears at the end of the paper.

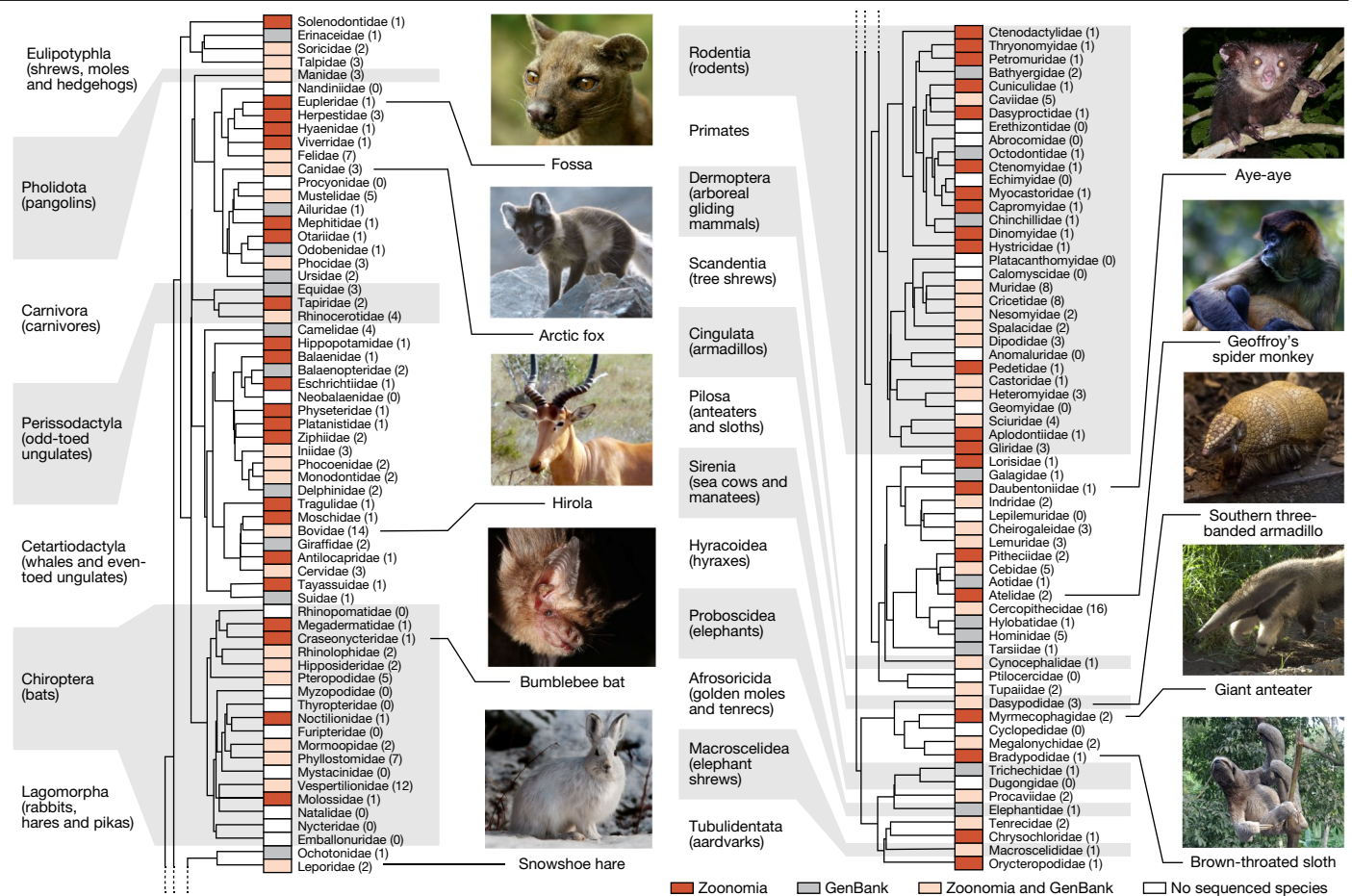


Fig. 1 | The Zoonomia Project brings the fraction of eutherian families that are represented by at least one assembly to 83%. Phylogenetic tree of the mammalian families in the Zoonomia Project alignment, including both our new assemblies and all other high-quality mammalian genomes publicly available in GenBank when we started the alignment (March 2018) (Supplementary Table 2). Tree topology is based on data from TimeTree (www.timetree.org)⁴⁷. Existing taxonomic classifications recognize a total of 127 extant families of eutherian mammal⁴⁸, including 43 families that were not previously represented in GenBank (red boxes) and 41 families with additional representative genome assemblies (pink boxes). Of the remaining families, 21 had GenBank genome assemblies but no Zoonomia Project assembly

dataset includes assemblies for two different dogs) and spanning about 110 million years of mammalian evolution (Supplementary Table 2). With a total evolutionary branch length of 16.6 substitutions per site, we expect only 191 positions in the human genome (0.000006%) to be identical across the aligned species owing to chance (false positives) rather than evolutionary constraint (Extended Data Table 2). We applied this same calculation to data from The Exome Aggregation Consortium (ExAC)—who analysed exomes for 60,706 humans¹⁴—and estimated that 88% of positions would be expected to have no variation. This illustrates the potential for relatively small cross-species datasets to inform human genetic studies—even for diseases driven by high-penetrance coding mutations, for which ExAC data are optimally powered¹⁵.

Biological insights from additional assemblies

The scope and species diversity in the Zoonomia Project supports evolutionary studies in many lineages. Previously published papers (discussed in the subsections below), and the demonstrated utility of existing comparative genomics resources^{16,17}, illustrate the benefits of

(grey boxes) and 22 had no representative genome assembly (white boxes). Parenthetical numbers indicate the number of species with genome assemblies in a given family. Image credits: fossa, Bertal/Wikimedia (CC BY-SA); Arctic fox, Michael Haferkamp/Wikimedia (CC BY-SA); hirola, JRProbert/Wikimedia (CC BY-SA); bumblebee bat, Sébastien J. Puechmaile (CC BY-SA); snowshoe hare, Denali National Park and Preserve/Wikimedia (public domain); aye-aye, TomJuneK/Wikimedia (CC BY-SA); Geoffroy's spider monkey, Patrick Gijbsers/Wikimedia (CC BY-SA); southern three-banded armadillo, Hedwig Storch/Wikimedia (CC BY-SA); giant anteater, Graham Hughes/Wikimedia (CC BY-SA); brown-throated sloth, Dick Culbert from Gibsons, B.C., Canada/Wikimedia (CC BY).

making newly generated genome assemblies and alignments accessible to all researchers without restrictions on use.

Speciation

Comparing our assembly for the endangered Mexican howler monkey (*Alouatta palliata mexicana*, a subspecies of the mantled howler monkey) with the Guatemalan black howler monkey (*Alouatta pigra*)—which has a neighbouring range—suggests that different forms of selection shape the reproductive isolation of the two species¹⁸. Initial divergence in allopatry was followed by positive selection on postzygotic isolating mechanisms, which offers empirical support for a speciation process that was first outlined by Dobzhansky in 1935¹⁹.

Protection from cancer

Using our assembly for the capybara (*Hydrochoerus hydrochaeris*) (a giant rodent), a previous publication²⁰ has identified positive selection on anti-cancer pathways, echoing previous reports²¹ that other large mammal species—the African and Asian elephants (*Loxodonta africana* and *Elephas maximus indicus*, respectively)—carry extra copies (retrogenes) of the tumour-suppressor gene *TP53*. This offers a possible

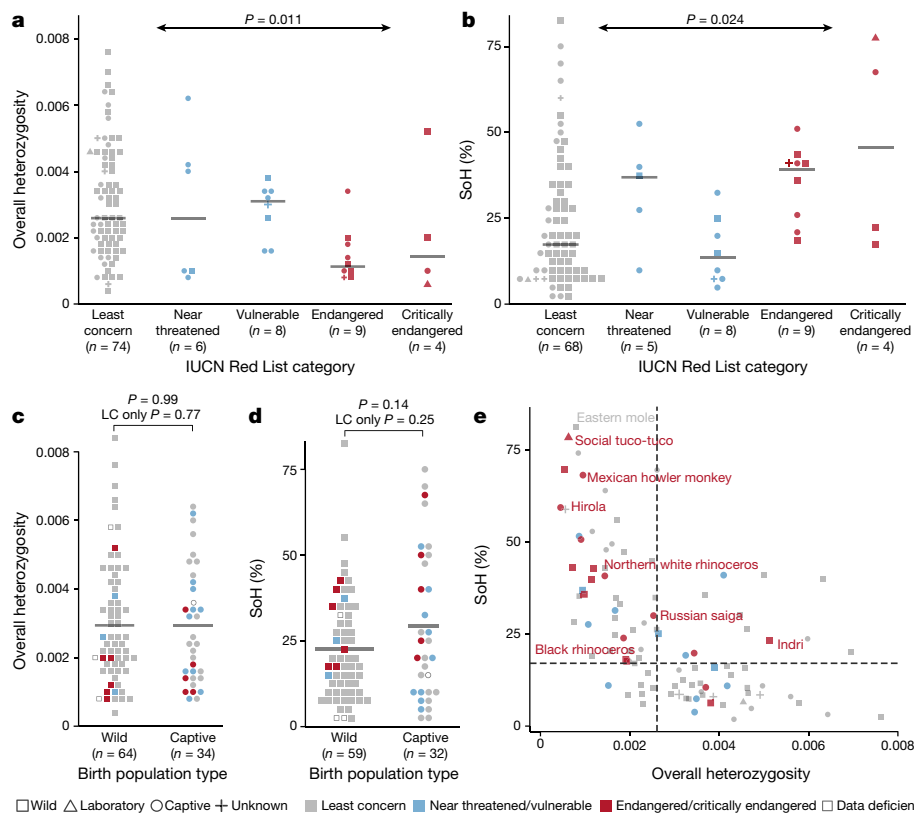


Fig. 2 | Genetic diversity varies across IUCN conservation categories.

a, b, Heterozygosity declines (**a**) and SoH value increases (**b**) with the level of concern for species conservation, as assessed by IUCN conservation categories. Horizontal grey lines indicate median. **c, d,** Comparing individuals sampled from wild and captive populations, we saw no statistically significant difference (independent samples *t*-test) in overall heterozygosity (**c**) or percent SoH (**d**), with similar means (horizontal grey lines) between types of birth

population. In **a–d**, there was a total of 105 species, with *n* for each tested category indicated on the x axis. Statistical tests were two-sided. LC, least concern. **e,** Overall heterozygosity and SoH values for all genomes analysed (including those with high allelic balance ratio; *n* = 124 species), with median SoH (17.1%, horizontal dashed line) and median overall heterozygosity (0.0026, vertical dashed line) for species categorized as least concern. Values for individuals from the seven critically endangered species are shown in red.

resolution to Peto’s paradox—the observation that cancer in large mammals is rarer than expected—and could reveal anti-cancer mechanisms.

Convergent evolution of venom

A previous publication²² has used our assembly for the Hispaniolan solenodon (*Solenodon paradoxus*) (Extended Data Fig. 2) to investigate venom production—a trait that is found in only a few eutherian lineages, including shrews and solenodons. They identified paralogous copies of a kallikrein 1 serine protease gene (*KLK1*) that together encode solenodon venom, and showed that the *KLK1* gene was independently co-opted for venom production in both solenodons and shrews, in an example of molecular convergence.

Informing biodiversity conservation strategies

A previous analysis²³ of our giant otter (*Pteronura brasiliensis*) assembly found low diversity and an elevated burden of putatively deleterious genetic variants, consistent with the recent population decline of this species through overhunting and habitat loss. The giant otter had fewer putatively deleterious variants than either the southern or northern sea otter (*Enhydra lutris nereis* and *E. lutris kenyoni*, respectively), which suggests that it has highest potential for recovery among these species if populations are protected.

Rapid assessment of species infection risk

Using the Zoonomia alignment and public genomic data from hundreds of other vertebrates, a previous publication²⁴ compared the structure of ACE2—the receptor for severe acute respiratory syndrome coronavirus 2 (SARS-CoV-2), the causative agent of coronavirus disease 2019

(COVID-19)—and identified 47 mammals that have a high or very high likelihood of being virus reservoirs, intermediate hosts or good model organisms for the study of COVID-19, and detected positive selection in the ACE2 receptor-binding domain that is specific to bats.

Genetic diversity and extinction risk

We next asked whether a reference genome from a single individual can help to identify populations with low genetic diversity to prioritize in efforts to conserve biodiversity. Diversity metrics reflect demographic history^{25,26}, and heterozygosity is lower in threatened species²⁷. This analysis was feasible because we used a single sequencing and assembly protocol for all DISCOVAR assemblies, which minimized variation in accuracy, completeness and contiguity due to the sequencing technology and the assembly process that would otherwise confound species comparisons.

We estimated genetic diversity for 130 of our DISCOVAR assemblies, each of which represented a different species (Supplementary Table 3). Four of these estimates failed during analysis. For the remaining 126 DISCOVAR assemblies, we calculated 2 metrics: (1) the fraction of sites at which the sequenced individual is heterozygous (overall heterozygosity); and (2) the proportion of the genome that resides in an extended region without any variation (segments of homozygosity (SoH)). The SoH measurement is designed for short-contiguity assemblies, in which scaffolds are potentially shorter than runs of homozygosity. Overall, heterozygosity and SoH values are correlated (Pearson correlation $r = -0.56, P = 1.8 \times 10^{-9}, n = 98$). Although overall heterozygosity is correlated with contig N50 values (Pearson correlation $r_{\text{het}} = -0.39$,

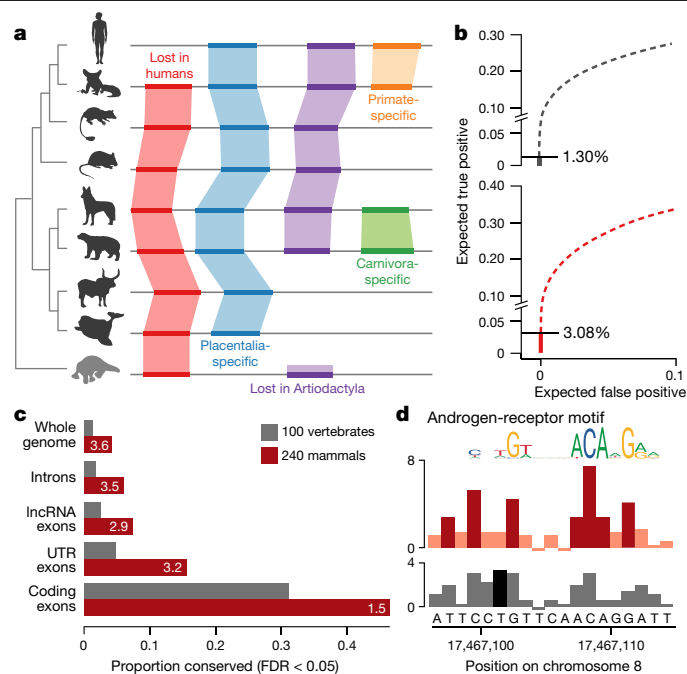


Fig. 3 | The Zoonomia alignment doubles the fraction of the human genome predicted to be under purifying selection at single-base-pair resolution.

a, Cactus alignments are reference-genome-free, enabling the detection of sequence that is absent from human (red) or other clades (purple), lineage-specific innovations (orange and green) and eutherian-mammal-specific sequence (blue). **b**, We compared phyloP predictions of conserved positions for a widely used 100-vertebrate alignment ($n = 100$ vertebrate species) (grey) to the Zoonomia alignment ($n = 240$ eutherian species) (red). The cumulative portion of the genome expected to be covered by true- versus false-positive calls is shown, starting from the highest confidence calls (solid line) and proceeding to calls with lower confidence (dashed lines); the horizontal line indicates the point at which the confidence level drops below an expected FDR of 0.05 (two-sided). **c**, A higher proportion of functionally annotated bases are detected as highly conserved (FDR < 0.05) in the Zoonomia alignment (red) than the 100-vertebrate alignment (grey), most notably in non-coding regions. lncRNA, long non-coding RNA; UTR, untranslated region. **d**, At a putative androgen-receptor binding site, phyloP scores predict that seven bases are under purifying selection (FDR < 0.05, two-sided) in the Zoonomia alignment (dark red), peaking in positions with the most information content in the androgen receptor JASPAR⁴⁹ motif, compared to one (dark grey) in the 100-vertebrate alignment, with scores at FDR > 0.05 shown in light red (top) and light grey (bottom).

$P_{\text{het}} = 4 \times 10^{-5}$, $n_{\text{het}} = 105$) (probably owing to the difficulty of assembling more heterozygous genomes²⁸), SoH values are not (Pearson correlation $r_{\text{SoH}} = 0.09$, $P_{\text{SoH}} = 0.38$, $n_{\text{SoH}} = 98$). Overall heterozygosity and SoH values are highly correlated between the lower- and high-contiguity versions of the upgraded assemblies (Pearson correlation $r_{\text{het}} = 0.999$, $P_{\text{het}} = 5 \times 10^{-7}$, $n_{\text{het}} = 7$; $r_{\text{SoH}} = 0.996$, $P_{\text{SoH}} = 1.4 \times 10^{-6}$, $n_{\text{SoH}} = 7$).

Genomic diversity varies significantly among species in different IUCN conservation categories, as measured by overall heterozygosity (Fig. 2a) and SoH values (Fig. 2b). SoH values increase ($P = 0.024$, $R^2 = 0.055$, $n = 94$) with increasing levels of conservation concern, whereas heterozygosity decreases ($P = 0.011$, $R^2 = 0.064$, $n = 101$). There is no significant difference between wild and captive populations in overall heterozygosity (Fig. 2c) or SoH values (Fig. 2d).

Unusual diversity values can suggest particular population demographics, although data from more than a single individual are needed to confirm these inferences. All seven critically endangered species have SoH values that are higher than the median for species categorized as of least concern (Fig. 2e). The genomes with the lowest heterozygosity and

highest SoH values were the social tuco-tuco (heterozygosity = 0.00063 and SoH = 78.7%), which was sampled from a small laboratory colony with only 12 founders²⁹, and the eastern mole (*Scalopus aquaticus*) (heterozygosity = 0.0008 and SoH = 81.3%), which was supplied by a professional mole catcher and was probably from a population that had experienced a bottleneck owing to pest control measures.

The correlation between diversity metrics and IUCN category is not explained by other species-level phenotypes. For species of least concern ($n = 75$), we assessed 21 phenotypes that are catalogued in the PanTHERIA³⁰ database for correlation with heterozygosity or SoH values. The most significant was between SoH value and litter size, a trait that has previously been shown to predict extinction risk³¹ ($P_{\text{SoH}} = 0.02$), but none is significant after Bonferroni correction (Extended Data Table 3).

Our inference that diversity trends lower in species at a higher risk of extinction comes from a small fraction (2.6%) of threatened mammals⁹. Whether this is a direct correlation with extinction risk or arises from an association between diversity and species-level phenotypes such as litter size, it suggests that valuable information can be gleaned from sequencing only a single individual. Should this pattern prove robust across more species, diversity metrics from a single reference genome could help to identify populations that are at risk—even when few species-level phenotypes are documented—and to prioritize species for follow-up at the population level.

Resources for biodiversity conservation

For each genome assembly, we catalogued all high-confidence variant sites (<http://broad.io/variants>) to support the design of cost-effective and accurate genetic assays that are usable even when the sample quality is low³²; such assays are often preferable to designing expensive custom tools, relying on tools from related species or sequencing random regions³³. The reference genomes themselves support the development of technologies such as using gene drives to control invasive species or pursuing ‘de-extinction’ through cloning and genetic engineering³⁴.

Our genomes have two notable limitations. We sequenced only a single individual for each species, which is insufficient for studying population origins, population structure and recent demographic events^{35,36}, and the shorter contiguity of our assemblies prevented us from analysing runs of homozygosity²⁶. This highlights a dilemma that faces all large-scale genomics initiatives: determining when the value of sequencing additional individuals exceeds the value of improving the reference genome itself.

Whole-genome alignment

We aligned the genomes of 240 species (our assemblies and other mammalian genomes that were released when we started the alignment) as part of a 600-way pan-amniote alignment using the Cactus alignment software³⁷ (Supplementary Table 2). Rather than aligning to a single anchor genome, Cactus infers an ancestral genome for each pair of assemblies (Fig. 3a). Consistent with our predictions, we have increased power to detect sequence constraint at individual bases relative to previous studies^{7,38}. We detect 3.1% of bases in the human genome to be under purifying selection in the eutherian lineage (false-discovery rate (FDR) < 5%), without using windowing or other means to integrate contextual information across neighbouring bases. This is more than double the number from the largest previous 100-vertebrate alignment³⁸ (Fig. 3b), with improvements being most notable in the non-coding sequence (Fig. 3c) and in the increased resolution of individual features (Fig. 3d). This represents a substantial proportion—but not all—of the 5 to 8% of the human genome that has previously been suggested to be under purifying selection^{7,39}.

Next steps

Using our alignment of 240 mammalian genomes, we are pursuing four key strategies of analysis. First, we aim to provide the largest eutherian

Analysis

phylogeny based on nuclear genomes by building a comprehensive phylogeny and time tree, including trees partitioned by functional annotations, mode of inheritance and long-term recombination rates. Second, we will produce a detailed map of evolutionary constraint, identifying highly conserved genomic regions, regions under accelerated evolution in particular lineages and changes that probably affect phenotype, leveraging functional data from ENCODE⁴⁰, GTEx⁴¹ and the Human Cell Atlas⁴². Third, we will use genotype–phenotype correlations to investigate patterns of constraint in regions associated with disease in humans, identify patterns of convergent adaptive evolution² and apply a forward genomics strategy to link functional elements to traits. Finally, we will explore the evolution of genome structure by mapping syntenic regions between genomes, identifying evolutionary breakpoints and characterizing the repeat landscape.

Conclusion

The Zoonomia Project has captured mammalian diversity at a high resolution, and is among the first of many projects that are underway to sequence, catalogue and characterize whole branches of the eukaryotic biodiversity of the Earth. On the basis of our experience, we propose the following principles for realizing the full value of large-scale comparative genomics.

First, we should prioritize sample collection. We must support field researchers who collect samples and understand species ecology and behaviour, develop strategies for sample collection that do not rely on bulky laboratory equipment or cold chains, develop technology for using non-invasive types of sampling and establish more repositories of renewable cell cultures¹⁰.

Second, we need accessible and scalable tools for computational analysis. Few research groups have access to the computational resources necessary for work with massive genomic datasets. We must address the shortage of skilled computational scientists, and design software and data-storage systems that make powerful computational pipelines accessible to all researchers.

Finally, we should promote rapid data-sharing. Data embargoes must not be permitted to delay analyses that directly benefit the conservation of endangered species, human health or progress in basic science. Genomic data should be shared as quickly as possible and without restrictions on use.

Numerous large-scale genome-sequencing efforts are now underway, including the Earth BioGenome Project⁴³, Genome 10K⁴⁴, the Vertebrate Genomes Project, Bat 1K⁴⁵, Bird 10K⁴⁶ and DNA Zoo. As the number of genomes grows, so too will the usefulness of comparative genomics in disease research and the development of therapeutic strategies. Preserving, rather than merely recording, the biodiversity of the Earth must be a priority. Through global scientific collaborations, and by making genomic resources available and accessible to all research communities, we can ensure that the legacy of genomics is not a digital archive of lost species.

Online content

Any methods, additional references, Nature Research reporting summaries, source data, extended data, supplementary information, acknowledgements, peer review information; details of author contributions and competing interests; and statements of data and code availability are available at <https://doi.org/10.1038/s41586-020-2876-6>.

1. Claussnitzer, M. et al. A brief history of human disease genetics. *Nature* **577**, 179–189 (2020).
2. Hiller, M. et al. A “forward genomics” approach links genotype to phenotype using independent phenotypic losses among related species. *Cell Rep.* **2**, 817–823 (2012).
3. Wasser, S. K. et al. Genetic assignment of large seizures of elephant ivory reveals Africa’s major poaching hotspots. *Science* **349**, 84–87 (2015).
4. Wright, B. et al. Development of a SNP-based assay for measuring genetic diversity in the Tasmanian devil insurance population. *BMC Genomics* **16**, 791 (2015).

5. Lappalainen, T., Scott, A. J., Brandt, M. & Hall, I. M. Genomic analysis in the age of human genome sequencing. *Cell* **177**, 70–84 (2019).
6. Kircher, M. et al. A general framework for estimating the relative pathogenicity of human genetic variants. *Nat. Genet.* **46**, 310–315 (2014).
7. Lindblad-Toh, K. et al. A high-resolution map of human evolutionary constraint using 29 mammals. *Nature* **478**, 476–482 (2011).
8. Finucane, H. K. et al. Partitioning heritability by functional annotation using genome-wide association summary statistics. *Nat. Genet.* **47**, 1228–1235 (2015).
9. IUCN. *The IUCN Red List of Threatened Species*. Version 2019-2 <https://www.iucnredlist.org> (2019).
10. Ryder, O. A. & Onuma, M. Viable cell culture banking for biodiversity characterization and conservation. *Annu. Rev. Anim. Biosci.* **6**, 83–98 (2018).
11. Weisenfeld, N. I. et al. Comprehensive variation discovery in single human genomes. *Nat. Genet.* **46**, 1350–1355 (2014).
12. Putnam, N. H. et al. Chromosome-scale shotgun assembly using an in vitro method for long-range linkage. *Genome Res.* **26**, 342–350 (2016).
13. Kim, J. et al. Reconstruction and evolutionary history of eutherian chromosomes. *Proc. Natl Acad. Sci. USA* **114**, E5379–E5388 (2017).
14. Lek, M. et al. Analysis of protein-coding genetic variation in 60,706 humans. *Nature* **536**, 285–291 (2016).
15. Balasubramanian, S. et al. Using ALoFT to determine the impact of putative loss-of-function variants in protein-coding genes. *Nat. Commun.* **8**, 382 (2017).
16. Meadows, J. R. S. & Lindblad-Toh, K. Dissecting evolution and disease using comparative vertebrate genomics. *Nat. Rev. Genet.* **18**, 624–636 (2017).
17. Cooper, G. M. & Shendure, J. Needles in stacks of needles: finding disease-causal variants in a wealth of genomic data. *Nat. Rev. Genet.* **12**, 628–640 (2011).
18. Baiz, M. D., Tucker, P. K., Mueller, J. L. & Cortés-Ortiz, L. X-linked signature of reproductive isolation in humans is mirrored in a howler monkey hybrid zone. *J. Hered.* **111**, 419–428 (2020).
19. Dobzhansky, T. & Dobzhansky, T. G. *Genetics and the Origin of Species* (Columbia Univ. Press, 1937).
20. Herrera-Álvarez, S., Karlsson, E., Ryder, O. A., Lindblad-Toh, K. & Crawford, A. J. How to make a rodent giant: genomic basis and tradeoffs of gigantism in the capybara, the world’s largest rodent. Preprint at <https://doi.org/10.1101/424606> (2018).
21. Abegglen, L. M. et al. Potential mechanisms for cancer resistance in elephants and comparative cellular response to DNA damage in humans. *J. Am. Med. Assoc.* **314**, 1850–1860 (2015).
22. Casewell, N. R. et al. Solenodon genome reveals convergent evolution of venom in eulipotyphlan mammals. *Proc. Natl Acad. Sci. USA* **116**, 25745–25755 (2019).
23. Beichman, A. C. et al. Aquatic adaptation and depleted diversity: a deep dive into the genomes of the sea otter and giant otter. *Mol. Biol. Evol.* **36**, 2631–2655 (2019).
24. Damas, J. et al. Broad host range of SARS-CoV-2 predicted by comparative and structural analysis of ACE2 in vertebrates. *Proc. Natl Acad. Sci. USA* **117**, 22311–22322 (2020).
25. Xue, Y. et al. Mountain gorilla genomes reveal the impact of long-term population decline and inbreeding. *Science* **348**, 242–245 (2015).
26. Ceballos, F. C., Joshi, P. K., Clark, D. W., Ramsay, M. & Wilson, J. F. Runs of homozygosity: windows into population history and trait architecture. *Nat. Rev. Genet.* **19**, 220–234 (2018).
27. Spielman, D., Brook, B. W. & Frankham, R. Most species are not driven to extinction before genetic factors impact them. *Proc. Natl Acad. Sci. USA* **101**, 15261–15264 (2004).
28. Vinson, J. P. et al. Assembly of polymorphic genomes: algorithms and application to *Ciona savignyi*. *Genome Res.* **15**, 1127–1135 (2005).
29. MacManes, M. D. & Lacey, E. A. The social brain: transcriptome assembly and characterization of the hippocampus from a social subterranean rodent, the colonial tuco-tuco (*Ctenomys sociabilis*). *PLoS ONE* **7**, e45524 (2012).
30. Jones, K. E. et al. PanTHERIA: a species-level database of life history, ecology, and geography of extant and recently extinct mammals. *Ecology* **90**, 2648 (2009).
31. Cardillo, M. Biological determinants of extinction risk: why are smaller species less vulnerable? *Anim. Conserv.* **6**, 63–69 (2003).
32. Natesh, M. et al. Empowering conservation practice with efficient and economical genotyping from poor quality samples. *Methods Ecol. Evol.* **10**, 853–859 (2019).
33. Lowry, D. B. et al. Breaking RAD: an evaluation of the utility of restriction site-associated DNA sequencing for genome scans of adaptation. *Mol. Ecol. Resour.* **17**, 142–152 (2017).
34. Shapiro, B. Pathways to de-extinction: how close can we get to resurrection of an extinct species? *Funct. Ecol.* **31**, 996–1002 (2017).
35. Benazzo, A. et al. Survival and divergence in a small group: the extraordinary genomic history of the endangered Apennine brown bear stragglers. *Proc. Natl Acad. Sci. USA* **114**, E9589–E9597 (2017).
36. Saremi, N. F. et al. Puma genomes from North and South America provide insights into the genomic consequences of inbreeding. *Nat. Commun.* **10**, 4769 (2019).
37. Armstrong, J. et al. Progressive Cactus is a multiple-genome aligner for the thousand-genome era. *Nature* <https://doi.org/10.1038/s41586-020-2871-y> (2020).
38. Haussler, M. et al. The UCSC genome browser database: 2019 update. *Nucleic Acids Res.* **47**, D853–D858 (2019).
39. Rands, C. M., Meader, S., Ponting, C. P. & Lunter, G. 8.2% of the human genome is constrained: variation in rates of turnover across functional element classes in the human lineage. *PLoS Genet.* **10**, e1004525 (2014).
40. ENCODE Project Consortium. An integrated encyclopedia of DNA elements in the human genome. *Nature* **489**, 57–74 (2012).
41. GTEx Consortium. Genetic effects on gene expression across human tissues. *Nature* **550**, 204–213 (2017).
42. Regev, A. et al. The human cell atlas. *eLife* **6**, e27041 (2017).
43. Lewin, H. A. et al. Earth BioGenome project: sequencing life for the future of life. *Proc. Natl Acad. Sci. USA* **115**, 4325–4333 (2018).
44. Koepfli, K.-P., Paten, B., the Genome 10K Community of Scientists & O’Brien, S. J. The Genome 10K project: a way forward. *Annu. Rev. Anim. Biosci.* **3**, 57–111 (2015).

45. Teeling, E. C. et al. Bat biology, genomes, and the Bat1K project: to generate chromosome-level genomes for all living bat species. *Annu. Rev. Anim. Biosci.* **6**, 23–46 (2018).
46. Feng, S. et al. Dense sampling of bird diversity increases power of comparative genomics. *Nature* <https://doi.org/10.1038/s41586-020-2873-9> (2020).
47. Kumar, S., Stecher, G., Suleski, M. & Hedges, S. B. TimeTree: a resource for timelines, timetrees, and divergence times. *Mol. Biol. Evol.* **34**, 1812–1819 (2017).
48. Wilson, D. E. & Reeder, D. M. (eds) *Mammal Species of the World. A Taxonomic and Geographic Reference* 3rd edn (Johns Hopkins Univ. Press, 2005).
49. Vlieghe, D. et al. A new generation of JASPAR, the open-access repository for transcription factor binding site profiles. *Nucleic Acids Res.* **34**, D95–D97 (2006).

Publisher's note Springer Nature remains neutral with regard to jurisdictional claims in published maps and institutional affiliations.



Open Access This article is licensed under a Creative Commons Attribution 4.0 International License, which permits use, sharing, adaptation, distribution and reproduction in any medium or format, as long as you give appropriate credit to the original author(s) and the source, provide a link to the Creative Commons license, and indicate if changes were made. The images or other third party material in this article are included in the article's Creative Commons license, unless indicated otherwise in a credit line to the material. If material is not included in the article's Creative Commons license and your intended use is not permitted by statutory regulation or exceeds the permitted use, you will need to obtain permission directly from the copyright holder. To view a copy of this license, visit <http://creativecommons.org/licenses/by/4.0/>.

© The Author(s) 2020

Zoonomia Consortium

Diane P. Genereux¹, Aitor Serres², Joel Armstrong³, Jeremy Johnson¹, Voichita D. Marinescu⁴, Eva Murén⁴, David Juan², Gill Bejerano^{5,6,7,8}, Nicholas R. Casewell⁹, Leona G. Chemnick¹⁰, Joana Damas¹¹, Federica Di Palma^{12,13}, Mark Diekhans³, Ian T. Fiddes³, Manuel Garber¹⁴, Vadim N. Gladyshev¹⁵, Linda Goodman^{15,16}, Wilfried Haerty¹³, Marlys L. Houck¹⁰, Robert Hubley¹⁷, Teemu Kivioja^{18,19}, Klaus-Peter Koepfli²⁰, Lukas F. K. Kuderna², Eric S. Lander^{1,21,22}, Jennifer R. S. Meadows⁴, William J. Murphy²³, Will Nash¹³, Hyun Ji Noh¹, Martin Nweeia^{24,25,26}, Andreas R. Pfenning²⁷, Katherine S. Pollard^{28,29,30}, David A. Ray³¹, Beth Shapiro^{32,33}, Arian F. A. Smit¹⁷, Mark S. Springer³⁴, Cynthia C. Steiner¹⁰, Ross Swofford¹, Jussi Taipale^{18,19,35}, Emma C. Teeling³⁶, Jason Turner-Maier¹, Jessica Alfoldi¹, Bruce Birren¹, Oliver A. Ryder^{10,37}, Harris A. Lewin^{11,38}, Benedict Paten³, Tomas Marques-Bonet^{2,39,40,41}, Kerstin Lindblad-Toh^{1,4,43} & Elinor K. Karlsson^{1,14,42,43} ✉

¹Broad Institute of MIT and Harvard, Cambridge, MA, USA. ²Institute of Evolutionary Biology (UPF-CSIC), PRBB, Barcelona, Spain. ³UC Santa Cruz Genomics Institute,

University of California Santa Cruz, Santa Cruz, CA, USA. ⁴Science for Life Laboratory, Department of Medical Biochemistry and Microbiology, Uppsala University, Uppsala, Sweden. ⁵Department of Biomedical Data Science, Stanford University, Stanford, CA, USA. ⁶Department of Computer Science, Stanford University, Stanford, CA, USA. ⁷Department of Developmental Biology, Stanford University, Stanford, CA, USA. ⁸Department of Pediatrics, Stanford University, Stanford, CA, USA. ⁹Centre for Snakebite Research and Interventions, Liverpool School of Tropical Medicine, Liverpool, UK. ¹⁰San Diego Zoo Global, Beckman Center for Conservation Research, San Diego, CA, USA. ¹¹The UC Davis Genome Center, University of California, Davis, Davis, CA, USA. ¹²Department of Biological Sciences, University of East Anglia, Norwich, UK. ¹³Earlham Institute, Norwich, UK. ¹⁴Program in Bioinformatics and Integrative Biology, University of Massachusetts Medical School, Worcester, MA, USA. ¹⁵Brigham and Women's Hospital, Harvard Medical School, Boston, MA, USA. ¹⁶Fauna Bio Incorporated, Emeryville, CA, USA. ¹⁷Institute for Systems Biology, Seattle, WA, USA. ¹⁸Department of Biochemistry, University of Cambridge, Cambridge, UK. ¹⁹Applied Tumor Genomics Research Program, University of Helsinki, Helsinki, Finland. ²⁰Smithsonian-Mason School of Conservation, Front Royal, VA, USA. ²¹Department of Biology, MIT, Cambridge, MA, USA. ²²Department of Systems Biology, Harvard Medical School, Boston, MA, USA. ²³Veterinary Integrative Biosciences, Texas A&M University, College Station, TX, USA. ²⁴Marine Mammal Program, Smithsonian Institution, Washington, DC, USA. ²⁵Restorative Dentistry and Biomaterials Sciences, Harvard School of Dental Medicine, Boston, MA, USA. ²⁶School of Dental Medicine, Case Western Reserve University, Cleveland, OH, USA. ²⁷Carnegie Mellon University, School of Computer Science, Department of Computational Biology, Pittsburgh, PA, USA. ²⁸Chan Zuckerberg Biohub, San Francisco, CA, USA. ²⁹Gladstone Institutes, San Francisco, CA, USA. ³⁰Department of Epidemiology and Biostatistics, Institute for Computational Health Sciences and Institute for Human Genetics, University of California, San Francisco, San Francisco, CA, USA. ³¹Department of Biological Sciences, Texas Tech University, Lubbock, TX, USA. ³²Department of Ecology and Evolutionary Biology, University of California, Santa Cruz, Santa Cruz, CA, USA. ³³Howard Hughes Medical Institute, University of California Santa Cruz, Santa Cruz, CA, USA. ³⁴Department of Evolution, Ecology and Organismal Biology, University of California, Riverside, Riverside, CA, USA. ³⁵Department of Medical Biochemistry and Biophysics, Karolinska Institutet, Stockholm, Sweden. ³⁶School of Biology and Environmental Science, University College Dublin, Dublin, Ireland. ³⁷Department of Evolution, Behavior, and Ecology, Division of Biology, University of California, San Diego, La Jolla, CA, USA. ³⁸Department of Evolution and Ecology, University of California, Davis, Davis, CA, USA. ³⁹Catalan Institution of Research and Advanced Studies (ICREA), Barcelona, Spain. ⁴⁰Institut Català de Paleontologia Miquel Crusafont, Universitat Autònoma de Barcelona, Barcelona, Spain. ⁴¹CNAG-CRG, Centre for Genomic Regulation (CRG), Barcelona Institute of Science and Technology (BIST), Barcelona, Spain. ⁴²Program in Molecular Medicine, University of Massachusetts Medical School, Worcester, MA, USA. ⁴³These authors contributed equally: Kerstin Lindblad-Toh, Elinor K. Karlsson. ✉e-mail: elinor@broadinstitute.org

Analysis

Methods

The number of samples (species) required to detect evolutionary conservation at a single base was estimated by applying a Poisson model of the distribution of substitution counts in the genome.

Species selection, sample shipping and regulatory approvals

Species were selected to maximize branch length across the eutherian mammal phylogeny, and to capture genomes of species from previously unrepresented eutherian families. Of 172 species initially selected for inclusion, we obtained sufficiently high-quality DNA samples for genome sequencing for 137. DNA samples from collaborating institutions were shipped to the Broad Institute ($n = 69$) or Uppsala University ($n = 68$). For samples received at the Broad Institute that were then sent to Uppsala, shipping approval was secured from the US Fish and Wildlife Service. Institutional Animal Care and Use Committee approval was not required.

Sample quality control, library construction and sequencing

DNA integrity for each sample was visualized via agarose gel (at the Broad Institute) or Agilent tape station (at Uppsala University). Samples passed quality control if the bulk of DNA fragments were greater than 5 kb. DNA concentration was then determined using Invitrogen Qubit dsDNA HS assay kit. For each of the samples that passed quality control, 1–3 μ g of DNA was fragmented on the Covaris E220 Instrument using the 400-bp standard programme (10% duty cycle, 140 PIP, 200 cycles per burst, 55 s). Fragmented samples underwent SPRI double-size selection ($0.55\times, 0.7\times$) followed by PCR-free Illumina library construction following the manufacturer's instructions (Kapa no. KK8232) using PCR-free adapters from Illumina (no. FC-121-3001). Final library fragment size distribution was determined on Agilent 2100 Bioanalyzer with High Sensitivity DNA Chips. Paired-end libraries were pooled, and then sequenced on a single lane of the Illumina HiSeq2500, set for Version 2 chemistry and 2×250 -bp reads. This yielded a total of mean 375 million (s.d. = 125 million) reads per sample.

Assembly and validation

For each species, we applied DISCOVAR de novo¹¹ (discovardenovo-52488) (<ftp://ftp.broadinstitute.org/pub/crd/DiscoverDeNovo/>) to assemble the 2×250 -bp read group, using the following command: `DiscoverDeNovo READS=[READFILE] OUT_DIR=[SPECIES_ID]/[SPECIES_ID].discover_files NUM_THREADS=24 MAX_MEM_GB=200G`.

Coverage for each genome was automatically calculated by DISCOVAR, with a mean coverage of $40.1\times$ (s.d. $\pm 14\times$). We assessed genome assembly, gene set and transcriptome completeness using Benchmarking Universal Single-Copy Orthologs (BUSCO), which provides quantitative measures on the basis of gene content from near-universal single-copy orthologues⁵⁰. BUSCO was run with default parameters, using the mammalian gene model set (mammalia_odb9, $n = 4,104$), using the following command: `python ./BUSCO.py -i [input fasta] -o [output_file] -l ./mammalia_odb9/ -m genome -c 1 -sp human`.

Median contig N50 for existing RefSeq assemblies was calculated using the assembly statistics for the most recent release of 118 eutherian mammals with RefSeq assembly accession numbers. Assemblies were all classified as either reference genome or representative genome. Assembly statistics were downloaded from the NCBI on 10 April 2019.

Genome upgrades. We selected genomes from each eutherian order without a pre-existing long-contiguity assembly on the basis of (1) whether the underlying assembly met the minimum quality threshold needed for HiRise upgrades; and (2) whether a second sample of sufficient quality could be obtained from that individual. All upgrades were done with Dovetail Chicago libraries and assembled with HiRise 2.1, as previously described⁵¹.

Estimating heterozygosity

Selection of assemblies for heterozygosity analysis. Heterozygosity statistics were calculated for all but four of our short read assemblies ($n = 126$) as well as eight Dovetail-upgraded genomes. Four failed because they were either too fragmented to analyse ($n = 3$) or because of undetermined errors ($n = 1$). One assembly was excluded because it was a second individual from a species that was already represented.

Heterozygosity calls. We applied the standard GATK pipeline with genotype quality banding to identify the callable fraction of the genome^{52,53}. First, we used samtools to subsample paired reads from the unmapped .bam files⁵⁴. After removing adaptor sequences from the selected reads, we used BWA-MEM to map reads to the reference genome scaffolds of >10 kb, removing duplicates using the PicardTools MarkDuplicates utility⁵⁵. We then called heterozygous sites using standard GATK-Haplotypecaller specifications, and with additional gVCF banding at 0, 10, 20, 30, 40, 50 and 99 qualities. We used the fraction of the genome with genotype quality >15 for subsequent analyses. For the lists of high-confidence variant sites, we include only heterozygous positions after filtering at $GQ > 20$, maximum DP < 100 , minimum DP > 6 , as described in the README file at <http://broad.io/variants>.

Inferring overall heterozygosity. To avoid confounding by sex chromosomes or complex regions, we excluded all scaffolds with less than 0.5 or greater than $2\times$ of the average sample read depth, then calculated global heterozygosity as the fraction of heterozygous calls over the whole callable genome.

Calling SoH. We estimated the proportion of the genome within SoH using a metric designed for genomes with scaffold N50 shorter than the expected maximum length of runs of homozygosity (our median scaffold N50 is 62 kb). We first split all scaffolds into windows with a maximum length of 50 kb, with windows ranging from 20 to 50 kb for scaffolds < 50 kb. For each window, we calculated the average number of heterozygous sites per bp. We discriminated windows with extremely low heterozygosity by using the Python 3.5.2 pomegranate package to fit a two-component Gaussian mixture model to the joint distribution of window heterozygosity, forcing the first component to be centred around the lower tail of the distribution and allowing the second to freely capture all the remaining heterozygosity variability^{56,57}. As heterozygosity cannot be negative, and normal distributions near zero can cross into negative values, we used the normal cumulative distribution function to correct the posterior distribution by the negative excess—effectively fitting a truncated normal to the first component. The final SoH value was calculated using the posterior maximum likelihood classification between both components. We saw no significant correlation between contig N50 and SoH (Pearson correlation = 0.055, $P = 0.57$, $n = 112$).

Assessing the effect of the percentage of callable genome. We assessed whether the percentage of the genome that was callable (Supplementary Table 3) was likely to affect our analysis. The callable percentage was correlated with heterozygosity ($r = -0.80$, $P < 2.2 \times 10^{-16}$, $n = 130$), and weakly with SoH values ($r = 0.18$, $P = 0.06$, $n = 112$). There is no significant difference in callable percentage among IUCN categories (analysis of variance $P = 0.98$, $n = 122$) or between captive and wild populations (t -test $P = 0.81$, $n = 120$).

Analysing patterns of diversity. We excluded two genomes with exceptionally high heterozygosity (heterozygosity > 0.02 ; > 5 s.d. above the mean). Both were of non-endangered species, and thus removing them made our determination of lower heterozygosity in endangered species more conservative. Of the remaining 124 genomes, we excluded 19 with allelic balance values that were more than one s.d. above the

mean (>0.36). Abnormally high allelic balance can indicate sequencing biases with potential for artefacts in estimates of heterozygosity and/or SoH. Our final dataset contains heterozygosity values for 105 genomes and SoH values for 98 genomes (Supplementary Table 3). For seven genomes, we were unable to estimate SoH because the two components of the Gaussian mixture model overlapped completely. To ask about a possible directional relationship between level of IUCN concern and overall heterozygosity or SoH, we applied regression using the IUCN category as an ordinal predictor. We also asked about the relationship of diversity metrics to a set of species-level phenotypes for which correlations were previously reported (Extended Data Table 3).

Alignment

The alignment was generated using the progressive mode of Cactus^{37,58}. The topology used for the guide tree of the alignment was taken from TimeTree⁴⁷; the branch lengths of the guide tree were generated by a least-squares fit from a distance matrix. The distance matrix was based on the UCSC 100-way phyloP fourfold-degenerate site tree³⁸ for those species that had corresponding entries in the 100-way tree. For species not present in the 100-way tree, distance matrix entries were more coarsely estimated using the distance estimated from Mash⁵⁹ to the closest relative included in the 100-way data.

Cactus does not attempt to fully resolve the gene tree when multiple duplications take place along a single branch, as there is an implicit restriction in Cactus that a duplication event be represented as multiple regions in the child species aligned to a single region in the parent species. This precludes representing discordance between the gene tree and species tree that could occur with incomplete lineage-sorting or horizontal transfer. However, the guide tree has a minimal effect on the alignment, with little difference between alignments with different trees—even when using a tree that is purposely wrong³⁷. Phenomena such as incomplete lineage sorting that affect a subset of species are unlikely to substantially affect the detection of purifying selection across the whole eutherian lineage described in Fig. 3.

The alignment was generated in several steps, on account of its large scale. First, a backbone alignment of several long contiguity assemblies was generated, using the genomes of two non-placental mammals (Tasmanian devil (*Sarcophilus harrisi*) and platypus (*Ornithorhynchus anatinus*)), to inform the reconstruction of the placental root. Next, separate clade alignments were generated for each major clade in the alignment: Euarchonta, Glires, Laurasiatheria, Afrotheria and Xenarthra. The roots of these clade alignments were then aligned to the corresponding ancestral genomes from the backbone, stitching these alignments together to create the final alignment. The process of aligning a genome to an existing ancestor is complex and further described in an accompanying Article that introduces the progressive mode of Cactus³⁷.

We created a neutral model for the conservation analysis using ancestral repeats detected by RepeatMasker⁶⁰ on the eutherian ancestral genome produced in the Cactus alignment (tRNA and low-complexity repeats were removed). To fit the neutral model, we used phyloFit from the PHAST⁶¹ package, using the REV (generalized reversible) model and EM optimization method. The training input was a MAF exported on columns from the set of ancestral repeats mentioned above. Because phyloFit does not support alignment columns that contain duplicates, if a genome had more than one sequence in a single alignment block, these were replaced with a single entry representing the consensus base at each column.

We extracted initial conservation scores using phyloP from the PHAST⁶¹ package on a MAF exported using human as a reference. We converted the phyloP scores (which represent log-scaled *P* values of acceleration or conservation) into *P* values, then into *q* values using the FDR-correction of Benjamini and Hochberg⁶². Any column with a resulting *q* value less than 0.05 was deemed significantly conserved or accelerated.

The alignment—as well as conservation annotations—are available at <https://cglgenomics.ucsc.edu/data/cactus/>.

Reporting summary

Further information on research design is available in the Nature Research Reporting Summary linked to this paper.

Data availability

The project website is <http://zoonomiaproject.org/>. Details of each Zoonomia genome assembly—including NCBI GenBank⁶³ accession numbers—are provided in Supplementary Table 1. Sequence data and genome assemblies are available at <https://www.ncbi.nlm.nih.gov/>. Variant lists for each species are provided at <http://broad.io/variants>. Further source data for Fig. 2 are provided in the Zoonomia GitHub repository (<https://doi.org/10.5281/zenodo.3887432>). The Cactus alignment is provided at <https://cglgenomics.ucsc.edu/data/cactus/>. A visualization of the alignments and phyloP data is available by loading our assembly hub into the UCSC browser⁶⁴ by copying the hub link https://comparative-genomics-hubs.s3-us-west-2.amazonaws.com/200m_hub.txt into the Track Hubs page. There are no restrictions on use. Source data are provided with this paper.

Code availability

The DISCOVAR de novo assembly code is available at https://github.com/broadinstitute/discovar_de_novo/releases/tag/v52488 (<https://doi.org/10.5281/zenodo.3870889>), the Cactus pipeline is available at <https://github.com/ComparativeGenomicsToolkit/cactus> (<https://doi.org/10.5281/zenodo.3873410>) and code for other analyses is available at <https://github.com/broadinstitute/Zoonomia/> (<https://doi.org/10.5281/zenodo.3887432>).

50. Simão, F. A., Waterhouse, R. M., Ioannidis, P., Kriventseva, E. V. & Zdobnov, E. M. BUSCO: assessing genome assembly and annotation completeness with single-copy orthologs. *Bioinformatics* **31**, 3210–3212 (2015).
51. Farré, M. et al. A near-chromosome-scale genome assembly of the gemsbok (*Oryx gazella*): an iconic antelope of the Kalahari desert. *Gigascience* **8**, giy162 (2019).
52. McKenna, A. et al. The genome analysis toolkit: a MapReduce framework for analyzing next-generation DNA sequencing data. *Genome Res.* **20**, 1297–1303 (2010).
53. DePristo, M. A. et al. A framework for variation discovery and genotyping using next-generation DNA sequencing data. *Nat. Genet.* **43**, 491–498 (2011).
54. Li, H. et al. The Sequence Alignment/Map format and SAMtools. *Bioinformatics* **25**, 2078–2079 (2009).
55. Li, H. & Durbin, R. Fast and accurate short read alignment with Burrows–Wheeler transform. *Bioinformatics* **25**, 1754–1760 (2009).
56. Benaglia, T., Chauveau, D., Hunter, D. & Young, D. mixtools: an R package for analyzing finite mixture models. *J. Stat. Softw.* **32**, 1–29 (2009).
57. R Core Team. *R: A Language and Environment for Statistical Computing*. <https://www.R-project.org/> (2019).
58. Paten, B. et al. Cactus: algorithms for genome multiple sequence alignment. *Genome Res.* **21**, 1512–1528 (2011).
59. Ondov, B. D. et al. Mash: fast genome and metagenome distance estimation using MinHash. *Genome Biol.* **17**, 132 (2016).
60. Smit, A. F. A., Hubley, R. & Green, P. *RepeatMasker Open-4.0*. <http://www.repeatmasker.org/> (2013–2015).
61. Hubisz, M. J., Pollard, K. S. & Siepel, A. PHAST and RPHAST: phylogenetic analysis with space/time models. *Brief. Bioinform.* **12**, 41–51 (2011).
62. Benjamini, Y. & Hochberg, Y. Controlling the false discovery rate: a practical and powerful approach to multiple testing. *J. R. Stat. Soc. B* **57**, 289–300 (1995).
63. Benson, D. A. et al. GenBank. *Nucleic Acids Res.* **41**, D36–D42 (2013).
64. Nguyen, N. et al. Comparative assembly hubs: web-accessible browsers for comparative genomics. *Bioinformatics* **30**, 3293–3301 (2014).
65. Karczewski, K. J. et al. The mutational constraint spectrum quantified from variation in 141,456 humans. *Nature* **581**, 434–443 (2020).
66. Pinheiro, E. C., Taddei, V. A., Migliorini, R. H. & Kettelhut, I. C. Effect of fasting on carbohydrate metabolism in frugivorous bats (*Artibeus lituratus* and *Artibeus jamaicensis*). *Comp. Biochem. Physiol. B Biochem. Mol. Biol.* **143**, 279–284 (2006).
67. Gordon, L. M. et al. Amorphous intergranular phases control the properties of rodent tooth enamel. *Science* **347**, 746–750 (2015).
68. Hindle, A. G. & Martin, S. L. Intrinsic circannual regulation of brown adipose tissue form and function in tune with hibernation. *Am. J. Physiol. Endocrinol. Metab.* **306**, E284–E299 (2014).
69. Stanford, K. I. et al. Brown adipose tissue regulates glucose homeostasis and insulin sensitivity. *J. Clin. Invest.* **123**, 215–223 (2013).
70. Chondronikola, M. et al. Brown adipose tissue improves whole-body glucose homeostasis and insulin sensitivity in humans. *Diabetes* **63**, 4089–4099 (2014).

Analysis

71. Saito, M. et al. High incidence of metabolically active brown adipose tissue in healthy adult humans: effects of cold exposure and adiposity. *Diabetes* **58**, 1526–1531 (2009).

Acknowledgements We thank the many individuals who provided samples and advice, including C. Adeno, C. Avila, E. Baitchman, R. Behringer, A. Boyko, M. Breen, K. Campbell, P. Campbell, C. J. Conroy, K. Cooper, L. M. Dávalos, F. Delsuc, D. Distel, C. A. Emerling, J. Fronczek, N. Gemmel, J. Good, K. He, K. Helgen, A. Hindle, H. Hoekstra, R. Honeycutt, P. Hulva, W. Israelsen, B. Kayang, R. Kennerley, M. Korody, D. N. Lee, E. Louis, M. MacManes, A. Misuraca, A. Mitelberg, P. Morin, A. Mouton, M. Murayama, M. Nachman, A. Navarro, R. Ogden, B. Pasch, S. Puechmaillie, T. J. Robinson, S. Rossiter, M. Ruedi, A. Seifert, S. Thomas, S. Turvey, G. Verbeylen and the late R. J. Baker. We also thank the Broad Institute Genomics Platform and SNP & SEQ Technology Platform (part of the National Genomics Infrastructure (NGI) Sweden and Science for Life Laboratory) and Swedish National Infrastructure for Computing (SNIC) at Uppmax. This project was funded by NIH NHGRI R01HG008742 (E.K.K., B.B., D.P.G., R.S., J.T.-M., J.J., H.J.N., B.P. and J. Armstrong), Swedish Research Council Distinguished Professor Award (K.L.-T., V.D.M., E.M. and J.R.S.M.), Swedish Research Council grant 2018-05973 (K.L.-T.), Knut and Alice Wallenberg Foundation (K.L.-T., V.D.M., E.M. and J.R.S.M.), Uppsala University (K.L.-T., V.D.M., E.M., J.R.S.M., J.J., J. Alfoldi and L.G.), Broad Institute Next10 (L.G.), Gladstone Institutes (K.S.P.), NIH NHGRI 5R01HG002939 (A.F.A.S. and R.H.), NIH NHGRI 5U24HG010136 (A.F.A.S. and R.H.), NIH NHGRI 5R01HG010485 (B.P. and M.D.), NIH NHGRI 2U41HG007234 (B.P., M.D. and J. Armstrong), NIH NIA 5PO1AG047200 (V.N.G.), NIH NIA 1UH2AG064706 (V.N.G.), BFMU2017-86471-P MINECO/FEDER, UE (T.M.-B.), Secretaria d'Universitats i Recerca and CERCA Programme del Departament d'Economia i Coneixement de la Generalitat de Catalunya GRC 2017 SGR 880 (T.M.-B.), Howard Hughes International Early Career (T.M.-B.), European Research Council Horizon 2020 no. 864203 (T.M.-B.), Obra Social 'La Caixa' (T.M.-B.), BBSRC BBS/E/T/000PR9818, BBS/E/T/ 000PR9783 (W.H. and W.N.), BBSRC Core Strategic Programme Grant BB/PO16774/1 (W.H., W.N. and F.D.), Sir Henry Dale Fellowship 200517/Z/16/Z jointly funded by the Wellcome Trust and the Royal Society (N.R.C.), FJCI-2016-29558 MICINN (D.J.), Prince Albert II Foundation of Monaco

and Canada, Global Genome Initiative, Smithsonian Institution (M.N.), European Research Council Research Grant ERC-2012-StG311000 (E.C.T.), Irish Research Council Laureate Award (E.C.T.), UK Medical Research Council MR/PO26028/1 (W.H. and W.N.), National Science Foundation DEB-1457735 (M.S.S.), National Science Foundation DEB-1753760 (W.J.M.), National Science Foundation IOS-2029774 (E.K.K. and D.P.G.), Robert and Rosabel Osborne Endowment (H.A.L. and J.D.), Swedish Research Council, FORMAS 221-2012-1531 (J.R.S.M.), NSF RoL: FELLS: EAGER: DEB 1838283 (D.A.R.) and Academy of Finland grant to Center of Excellence in Tumor Genetics Research no. 312042 (T.K. and J.T.).

Author contributions K.L.-T. conceived the project. J.J., V.D.M., E.M., N.R.C., L.G.C., J.D., V.N.G., M.L.H., K.-P.K., J.R.S.M., W.J.M., M.N., D.A.R., R.S., E.C.T., J. Alfoldi, O.A.R., H.A.L., K.L.-T. and E.K.K. contributed to the acquisition of the samples. J.J., V.D.M., E.M., J.D., L.G., K.-P.K., H.J.N., C.C.S., R.S., J.T.-M., J. Alfoldi, O.A.R., H.A.L., K.L.-T. and E.K.K. contributed to the production of the genome assemblies. D.P.G., A.S., J. Armstrong, J.J., D.J., I.T.F., L.F.K.K., H.A.L., T.M.-B., K.L.-T. and E.K.K. contributed to the data analysis. D.P.G., J.J., V.D.M., G.B., F.D.P., M.D., I.T.F., M.G., V.N.G., W.H., R.H., T.K., E.S.L., J.R.S.M., A.R.P., K.S.P., A.F.A.S., M.S.S., J.T., J. Alfoldi, B.B., O.A.R., H.A.L., B.P., T.M.-B., K.L.-T. and E.K.K. contributed to the design and conduct of the project. D.P.G., E.S.L., W.N., B.S., O.A.R., K.L.-T. and E.K.K. wrote the manuscript, with input from all other authors.

Competing interests L.G. is a co-founder of, equity owner in and chief technical officer at Fauna Bio Incorporated.

Additional information

Supplementary information is available for this paper at <https://doi.org/10.1038/s41586-020-2876-6>.

Correspondence and requests for materials should be addressed to E.K.K.

Peer review information *Nature* thanks Chris Ponting, Steven Salzberg, Guojie Zhang and the other, anonymous, reviewer(s) for their contribution to the peer review of this work.

Reprints and permissions information is available at <http://www.nature.com/reprints>.



Extended Data Fig. 1 | Notable traits in non-human mammals. Sequences from species with notable phenotypes can inform human medicine, basic biology and biodiversity conservation, but sample collection can be challenging. **a.** The Jamaican fruit bat (*Artibeus jamaicensis*) maintains constant blood glucose across intervals of fruit-eating and fasting⁶⁶, achieving homeostasis to a degree that is unknown in the treatment of human diabetes. **b.** The North American beaver (*Castor canadensis*) avoids tooth decay by incorporating iron rather than magnesium into tooth enamel, which yields an orange hue⁶⁷. **c.** The thirteen-lined ground squirrel (*Ictidomys tridecemlineatus*)

prepares for hibernation by rapidly increasing the thermogenic activity of brown fat⁶⁸, a process that—in humans—is connected to improved glucose homeostasis and insulin sensitivity⁶⁹⁻⁷¹. **d.** The tiny bumblebee bat (*Craseonycteris thonglongyai*) is among the smallest of mammals, making it a sparse source of DNA. **e.** The remote habitat of the very rare Amazon River dolphin (*Inia geoffrensis*) precludes collection of the high-molecular weight DNA. Image sources: Merlin D. Tuttle/Science Source (**a**); Stephen J. Krasemann/Science Source (**b**); Allyson Hindle (**c**); Sébastien J. Puechmaille (CC BY-SA) (**d**); M. Watson/Science Source (**e**).

Analysis



Extended Data Fig. 2 | Sample collection can be challenging, and sequencing methods must be selected to handle the sample quality. To enable the inclusion of species from across the eutherian tree (including from the 50% of mammalian families not represented in existing genome databases), the Zoonomia Project needed sequencing and assembly methods that produce reliable data from DNA collected in remote locations, sometimes in only modest quantities and often without benefit of cold chains for transport. **a**, For the marine species such as the narwhal (*Monodon monoceros*), simply accessing an individual in the wild can prove challenging. For example, to sample DNA from the near-threatened narwhal, M.N. and Inuit guide D. Angnatsiak camped on the edge of an ice floe between Pond Inlet and Bylot Island, at the northeastern tip of Baffin Island. After a narwhal was collected by Inuit hunters



as part of an annual hunt, hours of flensing were necessary for the collection of tissue samples. From left to right, F. McCann, H. C. Schmidt, F. Eichmiller, M.N., J. Orr (facing backward) and J. Orr (standing). **b**, For endangered species such as the Hispaniolan solenodon (*S. paradoxus*), sample collection must be designed to minimize stress to the individual, limiting the amount of DNA that can be collected²². To collect DNA from the endangered solenodon without imposing stress on individuals in the wild, N.R.C. turned to the world's only captive solenodons, which are housed off-exhibit at ZOODOM in the Dominican Republic. With help from veterinarians at the zoo, N.R.C. collected a small amount of blood from the rugged tail of the solenodon. Narwhal photograph by G. Freund, and courtesy of M.N. Solenodon photograph courtesy of L. Emery.

Extended Data Table 1 | The Zoonomia Project data includes 132 genome assemblies

n	Common Name	Species	Family	n	Common Name	Species	Family
EULIPTYPHLA (shrews, moles and hedgehogs)				RODENTIA (rodents)			
1	Hispaniolan solenodon	<i>Solenodon paradoxus (EN)</i>	Solenodontidae	69	Mountain beaver	<i>Aplodontia rufa</i>	Aplodontiidae
2	Indochinese shrew	<i>Crocidura indochinensis</i>	Soricidae	70	Desmarest's hutia	<i>Capromys pilorides</i>	Capromyidae
3	Eastern mole	<i>Scalopus aquaticus</i>	Talpidae	71	North American beaver	<i>Castor canadensis</i>	Castoridae
4	Gracile shrew-like mole	<i>Uropsilus gracilis</i>		72	Montane guinea pig	<i>Cavia tschudii</i>	Caviidae
CARNIVORA (carnivores)				73	Patagonian mara	<i>Dolichotis patagonum (NT)</i>	
5	Arctic fox	<i>Vulpes lagopus</i>	Canidae	74	Hispid cotton rat	<i>Sigmodon hispidus</i>	
6	Domestic dog (village dog)	<i>Canis lupus familiaris</i>		75	Muskkrat	<i>Ondatra zibethicus</i>	Cricetidae
7	Fossa	<i>Cryptoprocta ferax (VU)</i>	Eupleridae	76	Scorpion mouse	<i>Onychomys torridus</i>	
8	Black-footed cat	<i>Felis nigripes (VU)</i>	Felidae	77	Common gundi	<i>Ctenodactylus gundi</i>	Ctenodactylidae
9	Jaguar	<i>Panthera onca (NT)</i>		78	Social tuco-tuco	<i>Ctenomys sociabilis (CR)</i>	Ctenomyidae
10	Dwarf mongoose	<i>Helogale parvula</i>		79	Lowland paca	<i>Cuniculus paca</i>	Dasyproctidae
11	Meerkat	<i>Suricata suricatta</i>	Herpestidae	80	Central American agouti	<i>Dasyprocta punctata</i>	Dinomyidae
12	S Afr banded mongoose	<i>Mungos mungo</i>		81	Pacarana	<i>Dinomys branickii</i>	
13	Striped hyena	<i>Hyaena hyaena (NT)</i>	Hyaenidae	82	Gobi jerboa	<i>Allactaga bullata</i>	Dipodidae
14	Western spotted skunk	<i>Spilogale gracilis</i>	Mephitidae	83	Meadow jumping mouse	<i>Zapus hudsonius</i>	
15	Giant otter	<i>Pteronura brasiliensis (EN)</i>	Mustelidae	84	Edible dormouse	<i>Glis glis</i>	
16	Honey badger	<i>Mellivora capensis</i>		85	Hazel dormouse	<i>Muscardinus avellanarius</i>	Gliridae
17	California sea lion	<i>Zalophus californianus</i>	Otariidae	86	Woodland doormouse	<i>Graphiurus murinus</i>	
18	Northern elephant seal	<i>Mirounga angustirostris</i>	Phocidae	87	Pacific pocket mouse	<i>Perognathus longimembris</i>	Heteromyidae
19	Asian palm civet	<i>Paradoxurus hermaphroditus</i>	Viverridae	88	Stephen's kangaroo rat	<i>Dipodomys stephensi (VU)</i>	
PHOLIDOTA (pangolins)				89	Capybara	<i>Hydrochoerus hydrochaeris</i>	Cavidae
20	Tree pangolin	<i>Manis tricuspis* (VU)</i>	Manidae	90	Northern crested porcupine	<i>Hystrix cristata</i>	Hystricidae
PERISSODACTYLA (odd-toed ungulates)				91	Cairo spiny mouse	<i>Acomys cahirinus</i>	Muridae
21	Black rhinoceros	<i>Diceros bicornis* (CR)</i>	Rhinocerotidae	92	Mongolian jird	<i>Meriones unguiculatus</i>	
22	Northern white rhino	<i>Ceratotherium simum (CR)</i>		93	Coypu	<i>Myocastor coypus</i>	Myocastoridae
23	Malayan tapir	<i>Tapirus indicus (EN)</i>	Tapiridae	94	Gambian pouched rat	<i>Cricetomys gambianus</i>	Nesomyidae
24	South American tapir	<i>Tapirus terrestris (VU)</i>		95	South African springhare	<i>Pedetes capensis</i>	Pedetidae
CETARTIODACTYLA (whales and even-toed ungulates)				96	Dassie rat	<i>Petromus typicus</i>	Petromuridae
25	Pronghorn	<i>Antilocapra americana*</i>	Antilocapridae	97	Cape ground squirrel	<i>Xerus inauris</i>	Sciuridae
26	North Pacific right whale	<i>Eubalaena japonica (EN)</i>	Balaenidae	98	Hoary bamboo rat	<i>Rhizomys pruinosus</i>	Spalacidae
27	Hirola	<i>Beatragus hunteri (CR)</i>		99	Greater cane rat	<i>Thryonomys swinderianus</i>	Thryonomyidae
28	Nilgiri tahr	<i>Hemitragus hylocricus (EN)</i>		PRIMATES			
29	Peninsular bighorn sheep	<i>Ovis canadensis (EN)</i>	Bovidae	100	Geoffroy's spider monkey	<i>Ateles geoffroyi (EN)</i>	Atelidae
30	Russian saiga	<i>Saiga tatarica tatarica (CR)</i>		101	Mexican howler monkey	<i>Alouatta palliata mexicana (CR)</i>	
31	Siberian reindeer	<i>Rangifer tarandus (VU)</i>	Cervidae	102	Emperor tamarin	<i>Saguinus imperator</i>	Cebidae
32	Grey whale	<i>Eschrichtius robustus</i>	Eschrichtiidae	103	White-fronted capuchin	<i>Cebus albifrons</i>	Cebidae
33	Hippopotamus	<i>Hippopotamus amphibius* (VU)</i>	Hippopotamidae	104	De brazza's monkey	<i>Cercopithecus neglectus</i>	
34	Amazon river dolphin	<i>Inia geoffrensis (DD)</i>	Iniidae	105	N Plains gray langur	<i>Semnopithecus entellus</i>	
35	Pygmy sperm whale	<i>Kogia breviceps (DD)</i>	Kogidae	106	Patas monkey	<i>Erythrocebus patas</i>	Cercopithecidae
36	Narwhal	<i>Monodon monoceros</i>	Monodontidae	107	Proboscis monkey	<i>Nasalis larvatus (EN)</i>	
37	Narwhal	<i>Monodon monoceros</i>		108	Red-shanked douc	<i>Pygathrix nemaues (EN)</i>	
38	Siberian musk deer	<i>Moschus moschiferus* (VU)</i>	Moschidae	109	Coquerel's giant mouse lemur	<i>Mirza coquereli (EN)</i>	Cheirogaleidae
39	Harbor porpoise	<i>Phocoena phocoena</i>	Phocoenidae	110	Fat-tailed dwarf lemur	<i>Cheirogaleus medius</i>	
40	Indus river dolphin	<i>Platanista gangetica (EN)</i>	Platanistidae	111	Aye-aye	<i>Daubentonia madagascariensis (EN)</i>	Daubentonidae
41	La plata dolphin	<i>Pontoporia blainvilliei (VU)</i>	Iniidae	112	Indri	<i>Indri indri (CR)</i>	Indridae
42	Chacoan peccary	<i>Catagonus wagneri* (EN)</i>	Tayassuidae	113	Common brown lemur	<i>Eulemur fulvus (NT)</i>	Lemuridae
43	Java lesser chevrotain	<i>Tragulus javanicus* (DD)</i>	Tragulidae	114	Ring tailed lemur	<i>Lemur catta (EN)</i>	
44	Cuvier's beaked whale	<i>Ziphius cavirostris</i>	Ziphiidae	115	Sunda slow loris	<i>Nycticebus coucang (VU)</i>	Lorisidae
45	Sowerby's beaked whale	<i>Mesoplodon bidens (DD)</i>		116	White-eared titi	<i>Callicebus donacophilus</i>	Pitheciidae
CHIROPTERA (bats)				117	White-faced saki	<i>Pithecia pithecia</i>	
46	Bumblebee bat	<i>Craseonycteris thonglongyai (VU)</i>	Craseonycteridae	DERMOPTERA (arboreal gliding mammals)			
47	Cantor's leaf-nosed bat	<i>Hipposideros galeritus</i>	Hipposideridae	118	Sunda flying lemur	<i>Galeopterus variegatus*</i>	Cynocephalidae
48	Greater false vampire bat	<i>Megaderma lyra</i>	Megadermatidae	SCANDENTIA (tree shrews)			
49	Mexican free-tailed bat	<i>Tadarida brasiliensis</i>	Mormoopidae	119	Large treeshrew	<i>Tupaia tana</i>	Tupaiaidae
50	Ghost-faced bat	<i>Mormoops blainvilliei</i>	Mormoopidae	CINGULATA (armadillos)			
51	Greater bulldog bat	<i>Noctilio leporinus</i>	Noctilionidae	120	Screaming hairy armadillo	<i>Chaetophractus vellerosus</i>	Dasyproctidae
52	California leaf-nosed bat	<i>Macrotus californicus</i>		121	S. three-banded armadillo	<i>Tolypeutes matacus (NT)</i>	
53	Hairy big-eared bat	<i>Micronycteris hirsuta</i>		PILOSA (anteaters and sloths)			
54	Jamacian fruit-eating bat	<i>Artibeus jamaicensis</i>	Phyllostomidae	122	Brown-throated sloth	<i>Bradypus variegatus</i>	Bradypodidae
55	Seba's short-tailed bat	<i>Carollia perspicillata</i>		123	Linnaeus's two toed sloth	<i>Choloepus didactylus</i>	Megalonychidae
56	Stripe-headed round-eared bat	<i>Tonatia saurophila</i>		124	Giant anteater	<i>Myrmecophaga tridactyla (VU)</i>	Myrmecophagidae
57	Tailed tailless bat	<i>Anoura caudifer</i>		125	Southern tamandua	<i>Tamandua tetradactyla</i>	
58	Egyptian fruit bat	<i>Rousettus aegyptiacus</i>	Pteropodidae	HYRACOIDEA (hydraxes)			
59	Long-tongued fruit bat	<i>Macroglossus sobrinus</i>		126	Afr. yellow-spotted rock hyrax	<i>Heterohyrax brucei</i>	Procaviidae
60	Greater horseshoe bat	<i>Rhinolophus ferrumequinum</i>	Rhinolophidae	127	South African rock hyrax	<i>Procavia capensis*</i>	
61	Ashy-gray tube-nosed bat	<i>Murina feae</i>		AFROSORICIDA (golden moles and tenrecs)			
62	Common bent-wing bat	<i>Miniopterus schreibersii (NT)</i>		128	Cape golden mole	<i>Chrysochloris asiatica</i>	Chrysochloridae
63	Common pipistrelle	<i>Pipistrellus pipistrellus</i>		129	Lesser hedgehog tenrec	<i>Echinops telfairi†</i>	Tenrecidae
64	Eastern red bat	<i>Lasurus borealis</i>	Vespertilionidae	130	Talazac's shrew tenrec	<i>Microgale talazaci</i>	
65	Egyptian slit-faced bat	<i>Nycticeius humeralis</i>		MACROSCELIDEA (elephant shrews)			
66	Greater mouse-eared bat	<i>Myotis myotis</i>		131	Cape elephant shrew	<i>Elephantulus edwardii</i>	Macroscelididae
67	Pallid bat	<i>Antrozous pallidus</i>		TUBULIDENTATA (aardvarks) - first representative genome			
LAGOMORPHA (rabbits, hares, pikas)				132	Aardvark	<i>Orycteropus afer</i>	Orycteropodidae
68	Snowshoe hare	<i>Lepus americanus</i>	Leporidae				

These assemblies include 131 different species, with 2 narwhals (male and female), and 10 genomes upgraded to longer contiguity (including upgrade of an existing assembly for *E. telfairi*). Species of concern on the IUCN Red List are indicated as near-threatened (NT), vulnerable (V), endangered (EN) or critically endangered (CR).

*Upgraded to longer contiguity.

†Upgraded to longer contiguity using existing assembly.

Analysis

Extended Data Table 2 | Power to detect constraint across datasets

Dataset	Number of samples	Branch length	Expected fraction with no substitutions	Expected number of false positives
29 Mammals Project	29	4.9	7.5×10^{-3}	22,995,049
ExAC (33 megabases; exome only)	60,706	0.12	0.89	29,268,374
gnomAD v3	71,702	0.17	0.84	2,604,359,690
Zoonomia Project	240	16.6	6.2×10^{-8}	191

The expected number of variants conserved by chance (false positives) was estimated for four genomic resources (the 29 Mammals Project⁷ dataset, the human-only ExAC¹⁴ and gnomAD v.3⁶⁵ datasets, and the Zoonomia Project dataset) by applying a Poisson model of the distribution of substitution counts in the genome. Branch length for gnomAD was estimated by dividing 526,001,545 single-nucleotide variants by 3.088 gigabases (size of the human genome). Branch length for Zoonomia was measured as the number of substitutions per site in the phyloP analysis of the Cactus alignment.

Extended Data Table 3 | Diversity statistics are not correlated with other species-level phenotypes

Test	Phenotype	heterozygosity		segments of homozygosity		Description
		N	p	N	p	
Anova	12-1 HabitatBreadth	58	0.277	55	0.418	Number of habitat layers used by non-captive populations; Categories: above ground dwelling, aquatic, fossorial and ground dwelling
LM	15-1 LitterSize	64	0.094	59	0.018	Number of offspring born per litter per female
LM	26-1 GR Area km2	64	0.258	60	0.171	calculated using total extent of a species range with a global equal-area projection
LM	26-2 GR MaxLat dd	64	0.473	60	0.423	maximum latitudinal extent of each species range
LM	26-3 GR MinLat dd	64	0.850	60	0.773	minimum latitudinal extent of each species range
LM	26-4 GR MidRangeLat dd	64	0.038	60	0.179	median latitudinal extent of each species range
LM	26-5 GR MaxLong dd	64	0.655	60	0.694	maximum longitudinal extent of each species range
LM	26-6 GR MinLong dd	64	0.632	60	0.516	minimum longitudinal extent of each species range
LM	26-7 GR MidRangeLong dd	64	0.624	60	0.579	median longitudinal extent of each species range
LM	27-1 HuPopDen Min n-km2	64	0.567	60	0.268	minimum human population density
LM	27-2 HuPopDen Mean n-km2	64	0.342	60	0.330	mean human population density
LM	27-3 HuPopDen 5p n-km2	64	0.727	60	0.488	5th percentile human population density
LM	27-4 HuPopDen Change	64	0.372	60	0.107	mean rate of increase in human population density
LM	28-1 Precip Mean mm	64	0.092	60	0.433	mean monthly precipitation
LM	28-2 Temp Mean 01degC	64	0.098	60	0.063	mean monthly temperature (0.1°C)
LM	30-1 AET Mean mm	64	0.101	60	0.608	mean monthly AET (Actual Evapotranspiration Rate) from 1920 to 1980 (mm)
LM	30-2 PET Mean mm	64	0.078	60	0.154	mean monthly PET (Potential Evapotranspiration Rate) from 1920 to 1980
LM	5-1 AdultBodyMass g	66	0.228	61	0.823	Mass of adult (or age unspecified) live or freshly-killed specimens (excluding pregnant females)
Anova	6-1 DietBreadth	59	0.657	55	0.531	Number of dietary categories; for non-captive or non-provisioned populations; Categories: vertebrate, invertebrate, fruit, flowers/nectar/pollen, leaves/branches/bark, seeds, grass and roots/tubers
Anova	6-2 TrophicLevel	59	0.966	55	0.894	Trophic level of each species for non-captive or non-provisioned populations; Categories: (1) herbivore; (2) omnivore, or (3) carnivore
LM	9-1 GestationLen d	55	0.074	52	0.331	Length of time of non-inactive fetal growth
Anova	Family	35	0.088	33	0.421	Families with more than 1 representative species categorized as Least Concern, including: Canidae (2), Caviidae (2), Cebidae (2), Cercopithecidae (3), Cricetidae (2), Dipodidae (2), Herpestidae (3), Phyllostomidae (6), Pitheciidae (2), Procaviidae (2), Pteropodidae (2), Talpidae (2), Vespertilionidae (5)
Anova	Order	62	0.108	56	0.619	Orders with 4 or more species categorized as Least Concern, including Carnivora (9); Cetartiodactyla (5); Chiroptera (18); Primates (7); Rodentia (23).

All phenotypes in the PanTHERIA database³⁰ for which at least 75% of the 75 species of least concern had a value were included in the analysis. For continuous phenotypes, values were standardized to Z-scores before analysis (latitude was calculated as an absolute value) and correlation measured by fitting a linear model using the core R function lm. For categorical phenotypes with more than two categories, group means were compared using the core R function aov to fit an analysis of variance model. None was significant after Bonferroni correction for the number of traits considered (21).

Reporting Summary

Nature Research wishes to improve the reproducibility of the work that we publish. This form provides structure for consistency and transparency in reporting. For further information on Nature Research policies, see [Authors & Referees](#) and the [Editorial Policy Checklist](#).

Statistics

For all statistical analyses, confirm that the following items are present in the figure legend, table legend, main text, or Methods section.

n/a Confirmed

- The exact sample size (n) for each experimental group/condition, given as a discrete number and unit of measurement
- A statement on whether measurements were taken from distinct samples or whether the same sample was measured repeatedly
- The statistical test(s) used AND whether they are one- or two-sided
Only common tests should be described solely by name; describe more complex techniques in the Methods section.
- A description of all covariates tested
- A description of any assumptions or corrections, such as tests of normality and adjustment for multiple comparisons
- A full description of the statistical parameters including central tendency (e.g. means) or other basic estimates (e.g. regression coefficient) AND variation (e.g. standard deviation) or associated estimates of uncertainty (e.g. confidence intervals)
- For null hypothesis testing, the test statistic (e.g. F , t , r) with confidence intervals, effect sizes, degrees of freedom and P value noted
Give P values as exact values whenever suitable.
- For Bayesian analysis, information on the choice of priors and Markov chain Monte Carlo settings
- For hierarchical and complex designs, identification of the appropriate level for tests and full reporting of outcomes
- Estimates of effect sizes (e.g. Cohen's d , Pearson's r), indicating how they were calculated

Our web collection on [statistics for biologists](#) contains articles on many of the points above.

Software and code

Policy information about [availability of computer code](#)

Data collection

No software was used

Data analysis

DISCOVAR de novo (discoverdenovo-52488); BUSCO 2.0; HiRise 2.1; RStudio 1.2; R version 3.6.1; Samtools 1.8; BWA 0.7.17-r1188; GATK 3.6; Picard-Tools 2.21.3; Python 3.5.2 pomegranate package; ordPens package for R; Cactus (<https://www.biorxiv.org/content/10.1101/730531v3.full>); v1.5 PHAST; Custom python scripts for implementing SoH and heterozygosity analyses as described in methods.

For manuscripts utilizing custom algorithms or software that are central to the research but not yet described in published literature, software must be made available to editors/reviewers. We strongly encourage code deposition in a community repository (e.g. GitHub). See the Nature Research [guidelines for submitting code & software](#) for further information.

Data

Policy information about [availability of data](#)

All manuscripts must include a [data availability statement](#). This statement should provide the following information, where applicable:

- Accession codes, unique identifiers, or web links for publicly available datasets
- A list of figures that have associated raw data
- A description of any restrictions on data availability

Details on each Zoonomia Project genome assembly, including NCBI Genbank accession numbers, are in Supplementary Table 1. Sequence data and genome assemblies are available at <https://www.ncbi.nlm.nih.gov/>. Variant lists for each species are at broad.io/variants. Raw data for figure 3 is in Supplementary Table 2. There are no restrictions on data availability.

Field-specific reporting

Please select the one below that is the best fit for your research. If you are not sure, read the appropriate sections before making your selection.

Life sciences Behavioural & social sciences Ecological, evolutionary & environmental sciences

For a reference copy of the document with all sections, see [nature.com/documents/nr-reporting-summary-flat.pdf](https://www.nature.com/documents/nr-reporting-summary-flat.pdf)

Life sciences study design

All studies must disclose on these points even when the disclosure is negative.

Sample size	Sample size was determined based on evolutionary branch length calculations, as described in the manuscript.
Data exclusions	Diversity analysis: We excluded 2 genomes with high heterozygosity (> 6 standard deviations above the mean) and 17 genomes with allelic balance values more than one standard deviation above the mean. Exclusion criteria were established prior to analysis and described in Methods.
Replication	No replication. Study design required just one individual from each species be sequenced.
Randomization	Not relevant. This study did not involve experimental groups.
Blinding	Not relevant. This study did not involve experimental groups.

Reporting for specific materials, systems and methods

We require information from authors about some types of materials, experimental systems and methods used in many studies. Here, indicate whether each material, system or method listed is relevant to your study. If you are not sure if a list item applies to your research, read the appropriate section before selecting a response.

Materials & experimental systems

n/a	Involvement in the study
<input checked="" type="checkbox"/>	<input type="checkbox"/> Antibodies
<input checked="" type="checkbox"/>	<input type="checkbox"/> Eukaryotic cell lines
<input checked="" type="checkbox"/>	<input type="checkbox"/> Palaeontology
<input checked="" type="checkbox"/>	<input type="checkbox"/> Animals and other organisms
<input checked="" type="checkbox"/>	<input type="checkbox"/> Human research participants
<input checked="" type="checkbox"/>	<input type="checkbox"/> Clinical data

Methods

n/a	Involvement in the study
<input checked="" type="checkbox"/>	<input type="checkbox"/> ChIP-seq
<input checked="" type="checkbox"/>	<input type="checkbox"/> Flow cytometry
<input checked="" type="checkbox"/>	<input type="checkbox"/> MRI-based neuroimaging